Reproduced from Agronomy Journal. Published by American Society of Agronomy. All copyrights reserved.

Remote Sensing the Spatial Distribution of Crop Residues

C. S. T. Daughtry,* E. R. Hunt, Jr., P. C. Doraiswamy, and J. E. McMurtrey III

ABSTRACT

Management of plant litter or crop residues in agricultural fields is an important consideration for reducing soil erosion and increasing soil organic C. Current methods of quantifying crop residue cover are inadequate for characterizing the spatial variability of residue cover within fields and across large regions. Our objectives were to evaluate several spectral indices for measuring crop residue cover using ground-based and airborne hyperspectral data and to categorize soil tillage intensity in agricultural fields based on crop residue cover. Reflectance spectra of mixtures of crop residues, green vegetation, and soil were acquired over the 400- to 2500-nm wavelength region. High-altitude AVIRIS (Airborne Visible Infrared Imaging Spectrometer) data were also acquired near Beltsville, MD, in May 2000. Broad absorption features near 2100 and 2300 nm in the reflectance spectra of crop residues were associated with cellulose and lignin. These features were not evident in the spectra of green vegetation and soils. Crop residue cover was linearly related to the cellulose absorption index, which was defined as the relative depth of the 2100-nm absorption feature. Other spectral indices for crop residue were calculated and evaluated. The best spectral indices were based on relatively narrow (10–50 nm) bands in the 2000- to 2400-nm region, were linearly related to crop residue cover, and correctly identified tillage intensity classes in >90% of test agricultural fields. Regional surveys of soil management practices that affect soil conservation and soil C dynamics may be feasible using advanced multispectral or hyperspectral imaging systems.

Plant litter or crop residues on the soil surface play significant roles in the surface energy balance, net primary productivity, nutrient cycling, and C sequestration (Lal et al., 1999). Tillage accelerates soil erosion by increasing the soil's exposure to wind and rain and enhances C oxidation by increasing soil aeration, soil temperature, and soil–residue contact. As a result, the organic C content of most agricultural soils is much less than the organic C content of comparable native forest and grassland soils. Crop residue management, an integral component of most conservation tillage (CT) systems, includes selecting crops that produce sufficient quantities of residues and sowing cover crops to provide effective soil cover. The Conservation Technology Information Center (CTIC) has defined CT as any tillage and planting system that has >30% residue cover after planting, reduced tillage (RT) as 15 to 30% residue cover, and intensive tillage as <15% residue cover (CTIC, 2000). Long-term use of CT practices can lead to increased soil organic C, improved soil structure, and increased aggregation compared with intensively tilled soils (Rasmussen and Rohde, 1988). Process-based ecosystem models require information on tillage practices to adequately describe C and N dynamics in agricultural fields (Ma and Shaffer, 2001).

The standard technique used by the USDA-NRCS for measuring crop residue cover in individual fields is visual estimation along a line transect. This technique is time-consuming and prone to operator bias (Morrison et al., 1993; Corak et al., 1993). Rapid and accurate methods to quantify crop residue cover in individual fields are needed for management decisions. Regional assessments of crop residue cover and tillage practices in selected counties of the USA are compiled from annual roadside surveys of crop residue levels after planting (CTIC, 2000). These roadside surveys are subjective, and the techniques vary from county to county. Currently, no program exists for objectively monitoring crop residue cover or tillage intensity over broad areas.

Remote sensing could provide an efficient and objective method of obtaining information about crop residue cover and tillage intensity over large areas. Numerous spectral indices exploit the characteristic shape of the green vegetation spectrum by combining the low reflectance of the visible with the high reflectance of the near infrared to identify and quantify green vegetation. Rondeaux et al. (1996) grouped spectral vegetation indices into three broad categories: (i) *intrinsic spectral indices* that rely solely on measured reflectances in two or more bands, (ii) *soil-line-related indices* that use the generally linear relationship between visible and near infrared reflectances of bare soils to account for first-order soil background variation, and (iii) *atmospherically adjusted indices* that attempt to correct for radiation scattering produced by the atmospheric column. However, because crop residues lack the unique spectral signature of green vegetation in the 400- to 1000-nm wavelength region, discrimination between crop residues and soils is difficult using spectral vegetation indices (McMurtrey et al., 1993; Streck et al., 2002).

Other spectral indices have used the shortwave infrared wavelength bands of the Landsat Thematic Mapper (TM) to enhance the signal from crop residues. Examples include the Normalized Difference Tillage Index (NDTI; van Deventer et al., 1997), Normalized Difference Index (NDI; McNairn and Protz, 1993), and the Normalized Differential Senescent Vegetation Index (NDSVI; Qi et al., 2002). These indices are based on

USDA-ARS, Hydrol. and Remote Sens. Lab., Bldg. 007, Rm. 104, 10300 Baltimore Ave., Beltsville, MD 20705-2350 USA. Received 26 Nov. 2003. Remote Sensing. *Corresponding author (cdaughtry@hydrolab.arsusda.gov).

Published in Agron. J. 97:864–871 (2005).
doi:10.2134/agronj2003.0291
© American Society of Agronomy
677 S. Segoe Rd., Madison, WI 53711 USA

Abbreviations: ASTER, Advanced Spaceborne Thermal Emission and Reflection; AVIRIS, Airborne Visible Infrared Imaging Spectrometer; CAI, Cellulose Absorption Index; CT, conservation tillage; LCA, Lignin Cellulose Absorption (index); NDI, Normalized Difference Index; NDSVI, Normalized Differential Senescent Vegetation Index; NDTI, Normalized Difference Tillage Index; NDVI, Normalized Difference Vegetation Index; OSAVI, Optimized Soil-Adjusted Vegetation Index; RT, reduced tillage; TM, Thematic Mapper; VARI, Visible Atmospherically Resistant Index; VI_{green}, green vegetation index.

Reproduced from Agronomy Journal. Published by American Society of Agronomy. All copyrights reserved.

relative differences in broadband reflectance for soils and crop residues.

Alternative approaches for discriminating plant litter from soils are based on three broad absorption bands near 1730, 2100, and 2300 nm that are primarily associated with N, cellulose, and lignin, respectively (Curran, 1989; Elvidge, 1990). The strong absorption at 2100 nm appears in all compounds possessing alcoholic -OH groups, such as sugars, starch, and cellulose (Murray and Williams, 1988) and was clearly evident in the reflectance spectra of the dry crop residues (Daughtry, 2001; Streck et al., 2002) and dry, intact plant materials (Elvidge, 1990). The cellulose absorption feature was absent in the spectra of the soils. The Cellulose Absorption Index (CAI), which is an adaptation of the continuum-removal method (Kokaly and Clark, 1999), quantifies the relative depth of this absorption feature and discriminates crop residues from soils (Nagler et al., 2000). However, as the water content of plant litter increased, the absorption feature at 2100 nm was nearly obscured, and CAI was significantly reduced (Daughtry, 2001). Moisture had little effect on the CAI values of soils. The fraction of crop residue cover was linearly related to CAI in laboratory and field studies (Daughtry et al., 2004; Nagler et al., 2003). However, the CAI algorithm has not been evaluated over agricultural fields using aircraft or satellite hyperspectral images.

Our objectives were (i) to evaluate several spectral indices for estimating crop residue cover using ground-based reflectance data, (ii) to extend these indices using AVIRIS (Airborne Visible Infrared Imaging Spectrometer) data over a scene with a variety of land cover types, and (iii) to classify tillage intensity in agricultural fields based on spectral measures of crop residue cover.

MATERIALS AND METHODS

The USDA-ARS Beltsville Agricultural Research Center (BARC) located near Beltsville, MD, consists of >2000 ha of fields, pastures, and woodlands with an assortment of buildings, utilities, and roads. Surrounding BARC are residential, commercial, and light industrial areas on the north, south, and west and the Patuxent Wildlife Research Center to the east.

Field Spectra

Reflectance spectra of mixtures of green vegetation, crop residues, and soils were acquired with the spectroradiometer (FieldSpec Pro, Analytical Spectral Devices, Boulder, CO) over the 400- to 2500-nm wavelength region at 1-nm intervals. The 18° fore optics of the spectroradiometer and a 35-mm camera were aligned and mounted at 1.2 m above the soil surface. The diameter of the spectroradiometer's field of view at the soil surface was 0.38 m. For calibration, a 46-cm square Spectralon (Labsphere, North Sutton, NH) reference panel was placed in the field of view at 0.6 m from the optics, leveled, and measured in the same manner as the samples. Data were acquired under clear sky conditions in various corn (*Zea mays* L.), soybean [*Glycine max* (L.) Merr.], wheat (*Triticum aestivum* L.), tall fescue (*Festuca arundinacea* L.), and alfalfa (*Medicago sativa* L.) fields that had different tillage treatments. Reflectance factors were calculated (Robinson and Biehl, 1979). The color photograph acquired with each reflectance spectrum was scanned, and the fractions of green vegetation, crop residue, and soil in the field of view of the spectroradiometer were determined visually using a dot-grid overlay technique (Williams, 1979).

AVIRIS Data

High-altitude AVIRIS radiance data were acquired by the Jet Propulsion Laboratory (JPL) on 11 May 2000 at 1134 h over the Beltsville Agricultural Research Center and surrounding area. The spatial resolution (pixel size) of the AVIRIS image was 20 m. Spectral reflectance of a large asphalt tarmac (approximately 100 by 400 m) within the scene was acquired during the flight with the ASD spectroradiometer and a Spectralon panel. The spectroradiometer data were converted into the 224 AVIRIS bands using the year 2000 wavelength calibration provided by JPL. Pixel reflectance for the AVIRIS image was estimated from the radiance data using the Atmospheric Removal Program (ATREM 3.1). A one-point empirical correction of the AVIRIS image was applied using the mean reflectance spectrum of the asphalt tarmac measured during the flight. The AVIRIS images were analyzed and displayed using ENVI (Research Systems, Inc., Boulder, CO). Major water vapor absorption bands (AVIRIS bands at 1364–1464 nm and 1832–1991 nm) were removed from the data.

Broad land cover classes were identified by site visits and field records for 99 regions of interest within the AVIRIS scene. Fields classified as intensive tillage had been recently disked and were predominately bare soil with <15% crop residue cover. Conservation tillage fields were not tilled and had >30% cover from the previous crop. Fields classified as RT were lightly tilled or recently planted and had 15 to 30% crop residue cover. The green vegetation class included winter wheat (at heading stage), alfalfa, and hairy vetch (*Vicia villosa* L.) fields; orchardgrass (*Dactylis glomerata* L.) and tall fescue pastures, and conifer and deciduous trees. The mowed vegetation class included four alfalfa and grass fields that had been harvested for hay 1 to 2 d before the AVIRIS flight. The yellow vegetation class consisted of fields with standing dead and dying winter cover crops or cool-season weeds that had been recently sprayed with herbicides in preparation for no-till planting. Residential, industrial, and commercial areas within the scene were classified as nonagricultural.

Spectral Indices

The spectral bands of the Landsat TM, the Advanced Spaceborne Thermal Emission and Reflection (ASTER) radiometer (Abrams, 2000), and other indices were simulated using the narrow-band reflectance data obtained with either the ASD spectroradiometer or the AVIRIS. The intrinsic spectral index category was represented by the widely used Normalized Difference Vegetation Index (NDVI; Rouse et al., 1974),

$$\mathrm{NDVI} = (\mathrm{TM4} - \mathrm{TM3})/(\mathrm{TM4} + \mathrm{TM3}) \quad [1]$$

where TM3 and TM4 correspond to the reflectance in the Landsat TM Band 3 (630–690 nm) and Band 4 (760–900 nm), respectively. The green vegetation index ($\mathrm{VI}_{\mathrm{green}}$) described by Gitelson et al. (2002) was also included in the intrinsic category:

$$\mathrm{VI}_{\mathrm{green}} = (\mathrm{R}_{\mathrm{green}} - \mathrm{R}_{\mathrm{red}})/(\mathrm{R}_{\mathrm{green}} + \mathrm{R}_{\mathrm{red}}) \quad [2]$$

where $\mathrm{R}_{\mathrm{green}}$ is green reflectance in 546- to 556-nm band and $\mathrm{R}_{\mathrm{red}}$ is red reflectance in 620- to 670-nm band. The soil-line-related index category was represented by the Optimized Soil-Adjusted Vegetation Index (OSAVI; Rondeaux et al., 1996)

$$\mathrm{OSAVI} = (1 + 0.16)\,(\mathrm{TM4} - \mathrm{TM3})/(\mathrm{TM4} + \mathrm{TM3} + 0.16) \quad [3]$$

Reproduced from Agronomy Journal. Published by American Society of Agronomy. All copyrights reserved.

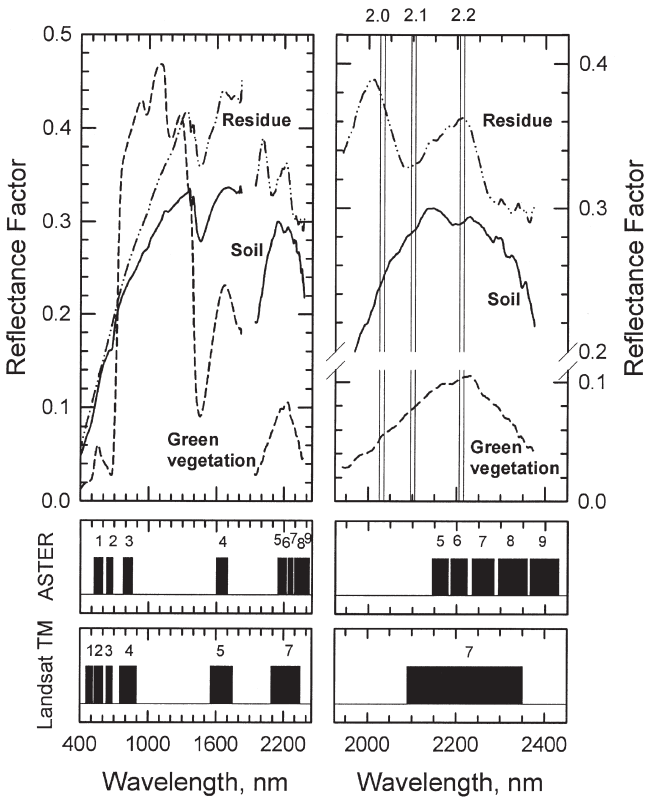

Fig. 1. Examples of field spectra for green vegetation, soil, and corn residue. Locations of Landsat-7 TM, ASTER, and CAI bands are shown.

where 0.16 is the optimized value to account for first-order soil background variation and TM3 and TM4 correspond to the reflectance in the Landsat TM Band 3 (630–690 nm) and Band 4 (760–900 nm), respectively. The atmospherically adjusted index category was represented by the Visible Atmospherically Resistant Index (VARI; Gitelson et al., 2002)

$$\mathrm{VARI} = (\mathrm{R_{green}} - \mathrm{R_{red}})/(\mathrm{R_{green}} + \mathrm{R_{red}} - \mathrm{R_{blue}}) \quad [4]$$

where R_{blue} is blue reflectance in 459- to 479-nm band, R_{green} is green reflectance in 546- to 556-nm band, and R_{red} is red reflectance in 620- to 670-nm band.

Four additional intrinsic spectral indices designed for detecting crop residues are the NDTI (van Deventer et al., 1997),

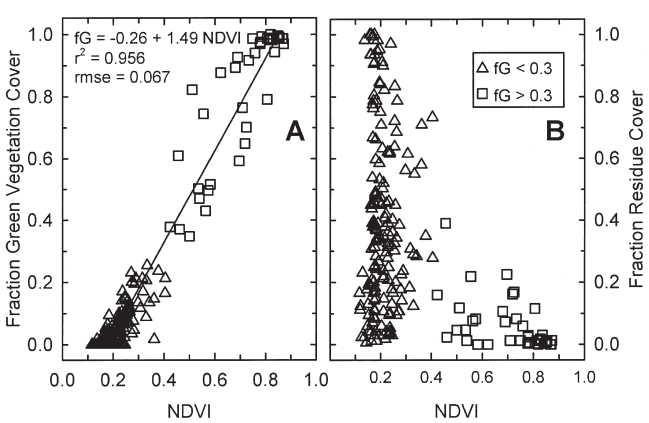

Fig. 2. Fraction of (A) green vegetation cover and (B) crop residue cover as a function of NDVI (n = 211). Squares indicate fraction of green vegetation cover (fG) > 0.3.

Table 1. Coefficients of determination (r^2) and root mean square errors (RMSE) for linear regressions of the fractions of residue cover as a function of various spectral indices. The two sets of regressions used either the entire data set (n = 211) or a subset (n = 171) that included only spectra with fractions of green vegetation (fG) < 0.3.

		All data (n = 211)		fG < 0.3 (n = 171)	
Eq. no.	Spectral index	r^2	RMSE	r^2	RMSE
1	NDVI	0.070	0.282	0.001	0.291
2	OSAVI	0.194	0.266	0.001	0.291
3	VI_{green}	0.209	0.264	0.032	0.287
4	VARI	0.220	0.262	0.056	0.283
5	NDTI	0.000	0.293	0.214	0.258
6	NDI5	0.182	0.265	0.174	0.265
7	NDI7	0.072	0.282	0.002	0.291
8	NDSVI	0.002	0.294	0.103	0.276
9	CAI	0.822	0.123	0.882	0.100
10	LCA	0.514	0.204	0.630	0.177

$$\mathrm{NDTI} = (\mathrm{TM5} - \mathrm{TM7})/(\mathrm{TM5} + \mathrm{TM7}) \quad [5]$$

the NDI (McNairn and Protz, 1993),

$$\mathrm{NDI5} = (\mathrm{TM4} - \mathrm{TM5})/(\mathrm{TM4} + \mathrm{TM5}) \quad [6]$$

$$\mathrm{NDI7} = (\mathrm{TM4} - \mathrm{TM7})/(\mathrm{TM4} + \mathrm{TM7}) \quad [7]$$

and the NDSVI (Qi et al., 2002)

$$\mathrm{NDSVI} = (\mathrm{TM5} - \mathrm{TM3})/(\mathrm{TM5} + \mathrm{TM3}) \quad [8]$$

where TM3, TM4, TM5, and TM7 correspond to reflectance in the Landsat TM Band 3 (630 nm), Band 4 (760–900 nm), Band 5 (1550–1750 nm), and Band 7 (2080–2350 nm), respectively.

Finally, two spectral indices based on the cellulose and lignin absorption features were evaluated. The CAI (Daughtry, 2001) was calculated as:

$$\mathrm{CAI} = 100[0.5(R_{2.0} + R_{2.2}) - R_{2.1}] \quad [9]$$

where $R_{2.0}$, $R_{2.1}$, and $R_{2.2}$ are the reflectance values in 10-nm bands centered at 2031, 2101, and 2211 nm, respectively. The Lignin Cellulose Absorption (LCA) index was defined as:

$$\mathrm{LCA} = 100[(\mathrm{ASTER6} - \mathrm{ASTER5}) + (\mathrm{ASTER6} - \mathrm{ASTER8})] \quad [10]$$

where ASTER5, ASTER6, and ASTER8 correspond to the ASTER (Abrams, 2000) Reflectance Band 5 (2145–2185 nm), Band 6 (2185–2225 nm), and Band 8 (2295–2365 nm), respectively. The LCA is the sum of the relative depths of the cellulose and lignin absorption features near 2100 and 2300 nm.

RESULTS AND DISCUSSION

Field Spectra

Typical reflectance spectra for green vegetation, crop residue, and soils are shown in Fig. 1. The soil and crop residue spectra have similar shapes and differ only in amplitude over the 400- to 1200-nm wavelength region. However, residues can be brighter or darker than the soils depending on many factors including species, moisture content, and age of the residue (Nagler et al., 2000). The breaks in the spectra are due to major water absorptions near 1450 and 1960 nm where the atmosphere absorbs nearly all of the incoming radiation. Broad absorption features near 2100 and 2300 nm are associated with cellulose and lignin in the crop residues (Curran, 1989; Elvidge, 1990). These absorption features are not

Reproduced from Agronomy Journal. Published by American Society of Agronomy. All copyrights reserved.

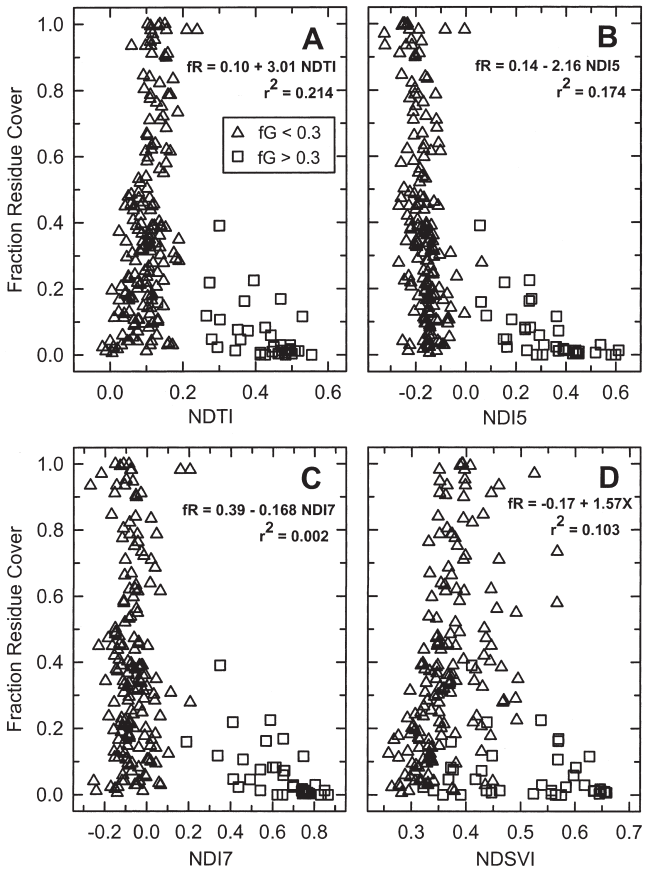

Fig. 3. Fraction of crop residue cover as a function of four Landsat TM spectral indices—(A) NDTI, (B) NDI5, (C) NDI7, and (D) NDSVI. Data with fractions of green vegetation cover (fG) > 0.3 were excluded from the regressions.

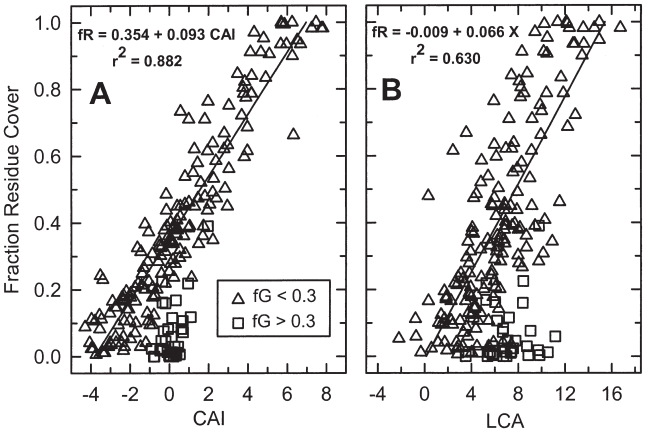

Fig. 4. Fraction of crop residue cover as a function of two spectral indices—(A) CAI and (B) LCA. Data with fractions of green vegetation cover (fG) > 0.3 were excluded from the regressions.

evident in the reflectance spectra of soil or green vegetation (Fig. 1).

Green vegetation cover is linearly related to NDVI (Fig. 2A), OSAVI, VI_{green}, and VARI (not shown) as numerous others have shown (e.g., Baret and Guyot, 1991; Gitelson et al., 2002). However, crop residue cover is not related to NDVI (Fig. 2B) or to any of the other green vegetation indices (Table 1). These spectral vegetation indices (Eq. [1] to [4]) were designed to enhance

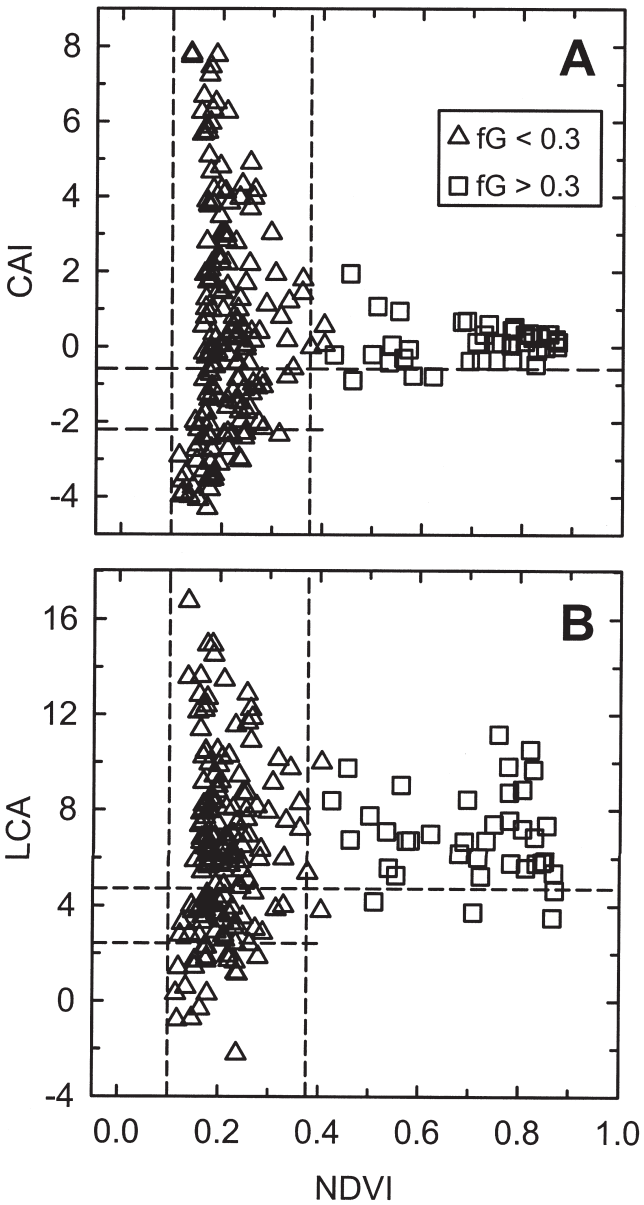

Fig. 5. Spectral indices (CAI and LCA) plotted as a function of NDVI for the ground-based ASD data (n = 211). The two vertical dashed lines indicate 0 and 0.3 fractions of green vegetation cover (fG). The two horizontal lines represent 0.15 and 0.30 fractions of crop residue cover (fR).

the green vegetation signal while minimizing the variation in background reflectance (Rondeaux et al., 1996). As a result, these green vegetation indices are inappropriate for assessing crop residue cover. Furthermore, crop residue cover was only weakly related to the crop residue/tillage indices NDTI, NDI5, NDI7, and NDSVI (Fig. 3A–3D; Table 1). The spectral bands of the Landsat TM are not well suited for discriminating crop residues from soil.

The subtle spectral differences associated with the cellulose and lignin absorption features are masked by broad spectral bands (Fig. 1). Crop residue cover is linearly related to CAI and LCA (Fig. 4A–4B). Excluding data with green vegetation fractions (fG) > 0.3 increased the coefficients of determination (r^2) and de-

Reproduced from Agronomy Journal. Published by American Society of Agronomy. All copyrights reserved.

creased the root mean square errors (RMSE) for these two indices (Table 1). Although the relatively narrow ASTER bands are located on the slopes and shoulders of the cellulose and lignin absorption features, the r^2 crop residue cover and LCA were greater than any of the spectral indices (Eq. [1], [2], and [5] to [8]) that used Landsat TM bands for quantifying crop residue cover (Table 1).

As the fractions of green vegetation increased, the scatter of each spectral index also increased (Fig. 3 and 4). The water in green vegetation significantly attenuated the reflectance signal from the absorption features in the shortwave infrared region (Murphy, 1995; Gao and Goetz, 1994) and significantly reduced CAI and LCA. The reflectance spectrum of a green leaf closely resembled the spectrum of wet cotton (*Gossypium hirsutum* L.) cellulose from 800 to 2500 nm (Elvidge, 1990) and was remarkably similar in shape and amplitude to the spectral of wet crop residue from 2000 to 2400 nm (Daughtry et al., 2004).

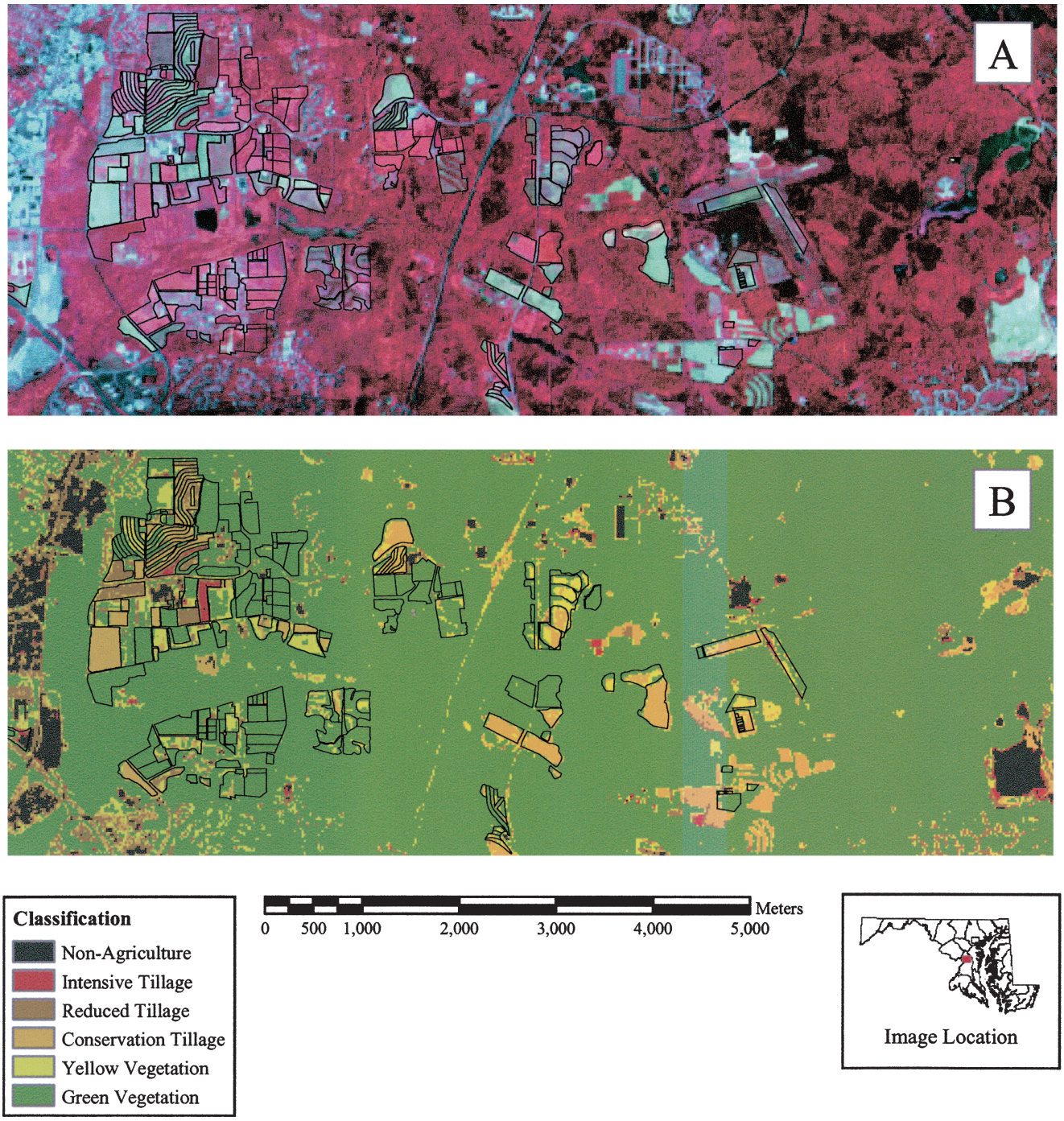

Fig. 6. (A) Color composite AVIRIS image with field boundaries outlined in black. Bands centered at 549, 646, and 827 nm were assigned blue, green, and red, respectively, in the image. (B) Tillage intensity classification of AVIRIS image using CAI and NDVI. Field boundaries are outlined in black.

Reproduced from Agronomy Journal. Published by American Society of Agronomy. All copyrights reserved.

In Fig. 5, CAI and LCA were each plotted as a function of NDVI. Based on the NDVI relationship from Fig. 2A, the two vertical dashed lines divide the feature space into three categories, i.e., (i) rocks and man-made materials, (ii) soils and crop residues, and (iii) yellow and green vegetation. Scenes with green vegetation cover fractions > 0.3 had NDVI values greater than bare soil or crop residue but had relatively low CAI and LCA values. The two horizontal lines, which represent 0.15 and 0.30 fractions of crop residue cover from Fig. 4, divide the feature space into three crop residue cover classes that correspond to intensive, reduced, and CT categories as defined by CTIC (2000). Thus, it appears possible that tillage intensity defined by crop residue cover can be inferred using these advanced spectral indices. However, when the fraction of green vegetation cover exceeds 0.3, crop residue cover and tillage intensity may be underestimated.

AVIRIS Data

The AVIRIS scene covered most of the USDA Beltsville Agricultural Research Center as well as surrounding residential, commercial, and industrial areas (Fig. 6A). Outlines of the agricultural fields and pastures within the Beltsville Agricultural Research Center were overlaid on the color composite image. Much of the vegetated area outside the fields is mixed hardwood and conifer woodlands and riparian wetlands. Examples of mean reflectance spectra for six cover types in the AVIRIS scene (Fig. 7) closely resemble the ground-based spectra (Fig. 1). The alfalfa, wheat (Fig. 7A), and trees (not shown) have typical green vegetation spectra with low visible reflectance and high near infrared reflectance. The mowed alfalfa and mowed grass spectra (Fig. 7B) are from fields that had been harvested for hay 1 to 2 d before the AVIRIS flight. The vegetation remaining in the mowed fields consisted primarily of 5- to 10-cm stems with very few green leaves over either bare soil or plant litter. In Fig. 7C, the yellow vegetation spectra are from two fields with winter cover crops [rye (*Secale cereale* L.)] and cool-season weeds (primarily wild mustards and annual grasses) that had been recently sprayed on different dates with a herbicide in preparation for no-till planting. Although the standing dead and dying vegetation obscured much of the underlying corn residue, the strong absorption feature at 2100 nm is evident in the both reflectance spectra. The corn and wheat residues (Fig. 7D) both exhibited the strong absorption feature near 2100 nm and the minor absorption feature near 2300 nm that were also observed in the ground-based spectra (Fig. 1).

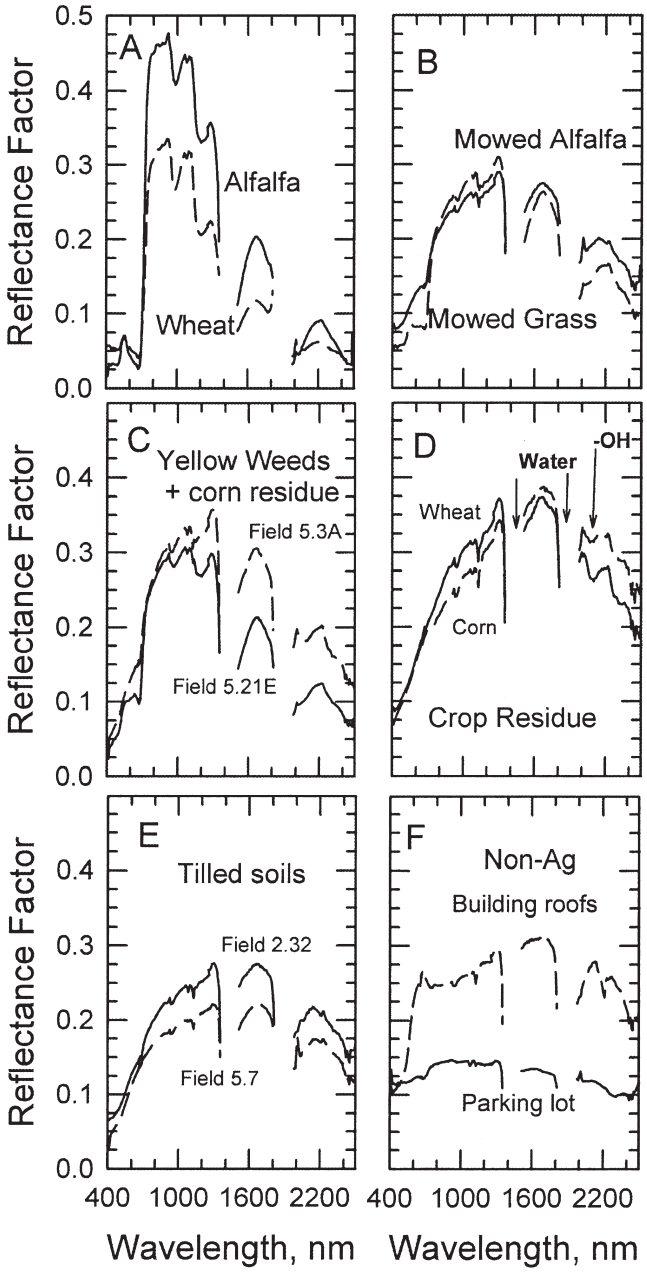

Fig. 7. AVIRIS spectra for six land cover types. The cellulose absorption feature (-OH) near 2100 nm is evident in B, C, and D (in increasing prominence) but not in other spectra. The two spectra represent the variability within each cover type.

The two spectra of tilled soils (Fig. 7E) were from different fields (and soil types) that were nearly bare soil (<15% residue cover) from disking several weeks ear-

Table 2. Mean spectral indices for regions of interest in the AVIRIS scene.

Class	*n*	NDVI	NDTI	NDI5	NDI7	NDSVI	CAI	LCA
Intensive till (IT)	2	0.122 d†	0.098 de	−0.131 c	−0.034 d	0.250 b	−1.348 d	2.30 d
Reduced till (RT)	4	0.191 d	0.139 cd	−0.057 c	0.082 cd	0.247 b	−0.466 c	4.39 c
Conservation till (CT)	30	0.202 cd	0.168 c	−0.091 c	0.077 cd	0.289 b	0.823 a	7.24 a
Yellow vegetation (YV)	12	0.346 b	0.229 b	0.076 b	0.297 b	0.274 b	0.529 ab	6.73 ab
Green vegetation (GV)	34	0.713 a	0.312 a	0.427 a	0.644 a	0.425 a	−0.033 bc	4.78 c
Mowed vegetation	4	0.303 bc	0.188 bc	−0.042 c	0.146 c	0.342 ab	−0.192 bc	5.26 bc
Nonagricultural RMSE	13	0.013 e	0.076 e	−0.086 c	−0.010 d	0.099 c	−1.920 d	1.06 d
		0.0902	0.0436	0.0999	0.1147	0.077	0.662	1.447

† Within each column, means followed by the same letter are not significantly different at $\alpha = 0.05$ using the Duncan multiple range test.

Reproduced from Agronomy Journal. Published by American Society of Agronomy. All copyrights reserved.

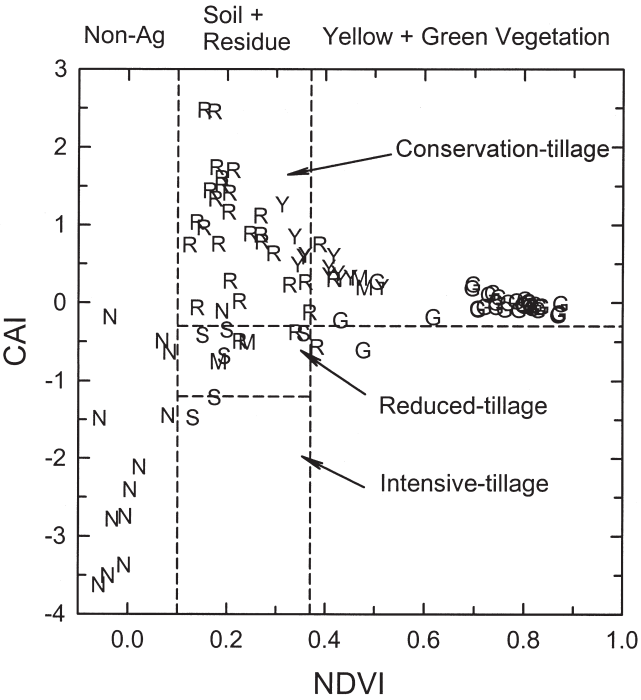

Fig. 8. Mean CAI vs. NDVI for 99 regions of interest in the AVIRIS image. Symbols refer to observed classes: C = conservation till, R = reduced till, T = intensive till, Y = yellow vegetation, G = green vegetation, M = mowed vegetation, and N = nonagricultural.

lier. The absorption features near 2100 and 2300 nm are absent in both spectra. Representative spectra for parking lots and commercial buildings (Fig. 7F) contrast sharply with spectra for agricultural areas. The sharp feature near 2200 nm is caused by a mineral absorption from the gravel used on the flat roof of a large industrial building. The parking lot was paved with asphalt and had some cars parked in it during the AVIRIS flight.

The mean spectral indices for seven land cover classes in the AVIRIS scene are shown in Table 2. The green and yellow vegetation classes differed significantly from the soil and residue classes for each of the Landsat TM–based indices. However, the differences among the three soil and residue classes were subtle and not successfully distinguished with the broadband spectral indices. The three relatively narrow-band spectral indices discriminated among the three levels of crop residue cover. The scatter plots of CAI and NDVI showed the clustering of cover types (Fig. 8) into broad and sometimes overlapping classes. Although the fractions of green vegetation and crop residue cover were not directly measured for the AVIRIS scene, the CAI and NDVI relationship for the AVIRIS data closely resembles the relationship shown in Fig. 5 for ground-based spectral data. The AVIRIS feature space was divided into three tillage intensity classes using CAI and three vegetation classes using NDVI (Fig. 8). Excluding the nonagricultural class, 72 of 86 (84%) agricultural regions of interest were correctly classified (Table 3). The cover crops in the yellow vegetation fields that had been sprayed with herbicides in preparation for no-till planting were in the process of becoming standing plant residue. The AVIRIS spectral indices classified 5 of the 12 yellow vegetation fields as high-residue fields (CT), which in retrospect may be more accurate than our observations. If the CT and yellow vegetation classes are combined (Table 4), classification accuracy for nongreen fields increased to 95% (46 of 48). Nevertheless, inferring tillage intensity solely from spectral observations on a single date can be misleading. For example, three of the four mowed alfalfa and grass fields that were harvested just before the AVIRIS flight were classified as low residue cover (RT) or yellow vegetation (Table 3). However, after a few weeks of regrowth, these fields would most likely have been correctly classified as green vegetation. Also, one corn field was classified as RT because the crop had been harvested for silage and very little crop residue remained on the soil surface.

When the entire image was classified using these spectral indices, more than 80% of the image was classified as green vegetation (Fig. 6B and Table 5). In the industrial and commercial (nonagricultural) areas, some pixels were classified as intensive tillage, RT, or CT based on the presence of senescent vegetation around the buildings and parking lots. Mixed pixels along major roadways in the scene were also classified as green or yellow vegetation or CT (brown vegetation). Accurate land use

Table 3. Classification matrix for regions of interest using CAI and NDVI values from the AVIRIS image. Italic numbers indicate correct classification. Overall classification accuracy of agricultural areas is 84%.

		Remotely sensed class					
Observed class	*n*	IT	RT	CT	YV	GV	Nonagric.
Intensive till (IT)	2	*2*	0	0	0	0	0
Reduced till (RT)	4	0	*4*	0	0	0	0
Conservation till (CT)	30	0	1	*26*	3	0	0
Yellow vegetation (YV)	12	0	0	5	*6*	1	0
Green vegetation (GV)	34	0	0	0	1	*33*	0
Mowed vegetation	4	0	2	0	1	1	0
Nonagricultural	13	0	0	1	0	0	*12*
Total	99						

Table 4. Classification matrix for combined regions of interest using CAI and NDVI values from the AVIRIS image. Italic numbers indicate correct classification. Overall classification accuracy of agricultural areas is 93%.

		Remotely sensed class			
Observed class	*n*	IT	RT	CT	GV
Intensive till (IT)	2	*2*	0	0	0
Reduced till (RT)	4	0	*4*	0	0
Conservation till (CT + YV)	42	0	1	*40*	1
Green vegetation (GV + mowed)	38	0	2	2	*34*
Total	86				

Table 5. Area of each land cover class determined using CAI and NDVI for the whole AVIRIS scene and for only the agricultural fields outlined in Fig. 6.

Remotely sensed class	Whole scene	BARC† fields
	ha	
Intensive till (IT)	21	7
Reduced till (RT)	187	30
Conservation till (CT + YV)	502	181
Green vegetation (GV)	3715	312
Nonagricultural	141	1
Total	4566	531

† BARC, Beltsville Agricultural Research Center.

Reproduced from Agronomy Journal. Published by American Society of Agronomy. All copyrights reserved.

classification is an important element for assessing crop residue cover and soil tillage intensity. For the agricultural fields shown in Fig. 6B, permanent pastures and winter crops (i.e., winter wheat, alfalfa, and hairy vetch) accounted for 59% of the area. Of the 218 ha designated for summer crops, 83% was classified as CT, 14% as RT, and only 3% as intensive tillage. This classification agreed closely with our ground observations and field records. Thus, it is possible to map crop residue cover and infer soil tillage intensity for agricultural fields using hyperspectral imaging systems. However, until hyperspectral images become readily available, multispectral sensors (e.g., ASTER) appear to have the appropriate bands for assessing crop residue cover. Additional evaluations of this concept are needed in regions with a more uniform mixture of intense tillage, RT, and CT practices.

ACKNOWLEDGMENTS

The authors thank Andrew Russ and Adam Booher for their technical assistance during this study. The AVIRIS imagery was acquired as part of a NASA Earth Observing System (EOS) validation program grant NAG5-6459.

REFERENCES

Abrams, M. 2000. ASTER: Data products for the high spatial resolution imager on NASA's EOS-AM1 platform. Int. J. Remote Sens. 21:847–861.

Baret, F., and G. Guyot. 1991. Potentials and limits of vegetation indices for LAI and APAR assessment. Remote Sens. Environ. 35:161–173.

Corak, S.J., T.C. Kaspar, and D.W. Meek. 1993. Evaluating methods for measuring residue cover. J. Soil Water Conserv. 48:700–704.

[CTIC] Conservation Technology Information Center. 2000. National survey of conservation tillage practices [Online]. Available at www.ctic.purdue.edu/CTIC/CRM.html (verified 1 Feb. 2005). CTIC, West Lafayette, IN.

Curran, P.J. 1989. Remote sensing of foliar chemistry. Remote Sens. Environ. 30:271–278.

Daughtry, C.S.T. 2001. Discriminating crop residues from soil by shortwave infrared reflectance. Agron. J. 93:125–131.

Daughtry, C.S.T., E.R. Hunt, Jr., and J.E. McMurtrey III. 2004. Assessing crop residue cover using shortwave infrared reflectance. Remote Sens. Environ. 90:126–134.

Elvidge, C.D. 1990. Visible and near infrared reflectance characteristics of dry plant materials. Int. J. Remote Sens. 10:1775–1795.

Gao, B.C., and A.F.H. Goetz. 1994. Extraction of dry leaf spectral features from reflectance spectra of green vegetation. Remote Sens. Environ. 47:369–374.

Gitelson, A.A., Y.J. Kaufman, R. Stark, and D. Rundquist. 2002. Novel algorithms for remote estimation of vegetation fraction. Remote Sens. Environ. 80:76–87.

Kokaly, R.F., and R.N. Clark. 1999. Spectroscopic determination of leaf biochemistry using band-depth analysis of absorption features and stepwise multiple linear regression. Remote Sens. Environ. 67:267–287.

Lal, R., J.M. Kimble, R.F. Follett, and C.V. Cole. 1999. The potential of U.S. cropland to sequester carbon and mitigate the greenhouse effect. Lewis Publ., Boca Raton, FL.

Ma, L., and M.J. Shaffer. 2001. A review of carbon and nitrogen processes in nine U.S. soil nitrogen dynamics models. p. 55–102. *In* M.J. Shaffer, L. Ma, and S. Hansen (ed.) Modeling carbon and nitrogen dynamics for soil management. Lewis Publ., Boca Raton, FL.

McMurtrey, J.E., E.W. Chappelle, C.S.T. Daughtry, and M.S. Kim. 1993. Fluorescence and reflectance of crop residue and soil. J. Soil Water Conserv. 48:207–213.

McNairn, H., and R. Protz. 1993. Mapping corn residue cover on agricultural fields in Oxford County, Ontario, using Thematic Mapper. Can. J. Remote Sens. 19:152–159.

Morrison, J.E., Jr., C. Huang, D.T. Lightle, and C.S.T. Daughtry. 1993. Residue cover measurement techniques. J. Soil Water Conserv. 48:479–483.

Murphy, R.J. 1995. The effects of surficial vegetation cover on mineral absorption feature parameters. Int. J. Remote Sens. 16:2153–2164.

Murray, I., and P.C. Williams. 1988. Chemical principles of near-infrared technology. p. 17–34. *In* P. Williams and K. Norris (ed.) Near-infrared technology in the agricultural and food industries. Am. Assoc. of Cereal Chemists, St. Paul, MN.

Nagler, P.L., C.S.T. Daughtry, and S.N. Goward. 2000. Plant litter and soil reflectance. Remote Sens. Environ. 71:207–215.

Nagler, P.L., Y. Inoue, E.P. Glenn, A.L. Russ, and C.S.T. Daughtry. 2003. Cellulose absorption index (CAI) to quantify mixed soil–plant litter scenes. Remote Sens. Environ. 87:310–325.

Qi, J., R. Marsett, P. Heilman, S. Biedenbender, M.S. Moran, D.C. Goodrich, and M. Weltz. 2002. RANGES improves satellite-based information and land cover assessments in Southwest United States. EOS Trans. Am. Geophys. Union 83(51):601–606.

Rasmussen, P.E., and C.R. Rohde. 1988. Long-term tillage and nitrogen fertilization effects on organic N and C in a semi-arid soil. Soil Sci. Soc. Am. J. 44:596–600.

Robinson, B.F., and L.L. Biehl. 1979. Calibration procedures for measurements of reflectance factor in remote sensing field research. Proc. Soc. Photo-Opt. Instrum. Eng. 196:16–26.

Rondeaux, G., M. Steven, and F. Baret. 1996. Optimization of soil-adjusted vegetation indices. Remote Sens. Environ. 55:95–107.

Rouse, J.W., R.H. Haas, Jr., J.A. Schell, and D.W. Deering. 1974. Monitoring vegetation systems in the Great Plains with ERTS. p. 309–317. *In* Proc. ERTS-1 Symp., 3rd, Greenbelt, MD. 10–15 Dec. 1973. Vol. 1. NASA SP-351. NASA, Washington, DC.

Streck, N.A., D. Rundquist, and J. Connot. 2002. Estimating residual wheat dry matter from remote sensing measurements. Photogramm. Eng. Remote Sens. 68:1193–1201.

van Deventer, A.P., A.D. Ward, P.H. Gowda, and J.G. Lyon. 1997. Using Thematic Mapper data to identify contrasting soil plains and tillage practices. Photogramm. Eng. Remote Sens. 63:87–93.

Williams, T.H.L. 1979. An error analysis of the photographic technique for measuring percent vegetative cover. Soil Sci. Soc. Am. J. 43:578–582.